Study of Bose-Einstein Correlations for Pions Produced in *pp* Collisions at 400 GeV/c (LEBC-EHS Collaboration)

Shoichi KITAMURA

M.Aguilar-Benitez, W.W.M.Allison, A.A.Batalov, E.Castelli, P.Checchia, N.Colino, R.Contri, A.De Angelis, A.De Roeck, N.De Seriis, E.A.De Wolf, J.Duboc, A.M.Endler, P.F.Ermolov, S.Falciano, Y.V.Fisyak, F.Fontanelli, S.Ganguli, U.Gasparini, S.Gentile, A.Gurtu, R.Hamatsu, J.J.Hernandez, T.Hirose, S.O.Holmgren, J.Hrubec, M.Iori, K.E.Johansson, M.I.Josa, E.P.Kistenev, A.Michalon, M.E.Michalon-Mentzer, M.Mazzucato, L.Montanet, R.Monge, H.K.Nguyen, H.Novak, L.C.Oliveira, V.M.Perevoztchikov, P.Pilette, P.Poropat, A.Poppleton, H.Rohringer, S.Saran, J.M.Salicio, M.Sessa, E.K.Shabalina, F.Simonetto, N.A.Sotnikova, S.Squarcia, V.A.Stopchenko, U.Trevisan, C.Troncon, F.Verbeure, J.V.Yarba, G.Zumerle

Bulletin of Tokyo Metropolitan College of Allied Medical Sciences

No.8

March 1995

〔原　著〕

Study of Bose-Einstein Correlations for Pions Produced in *pp* Collisions at 400 GeV/c (LEBC-EHS Collaboration)

Shoichi KITAMURA

M.Aguilar-Benitez[6], W.W.M.Allison[9], A.A.Batalov[14], E.Castelli[18], P.Checchia[10], N.Colino[6], R.Contri[5], A.De Angelis[10], A.De Roeck[1], N.De Seriis[12], E.A.De Wolf[1], J.Duboc[11], A.M.Endler[13], P.F.Ermolov[8], S.Falciano[12], Y.V.Fisyak[8], F.Fontanelli[5], S.Ganguli[3], U.Gasparini[10], S.Gentile[12], A.Gurtu[3], R.Hamatsu[17], J.J.Hernandez[6], T.Hirose[17], S.O.Holmgren[16], J.Hrubec[19], M.Iori[12], K.E.Johansson[16], M.I.Josa[6], E.P.Kistenev[14], A.Michalon[15], M.E.Michalon-Mentzer[15], M.Mazzucato[10], L.Montanet[4], R.Monge[5], H.K.Nguyen[11], H.Novak[2], L.C.Oliveira[13], V.M.Perevoztchikov[14], P.Pilette[7], P.Poropat[18], A.Poppleton[4], H.Rohringer[19], S.Saran[3], J.M.Salicio[6], M.Sessa[18], E.K.Shabalina[8], F.Simonetto[10], N.A.Sotnikova[8], S.Squarcia[5], V.A.Stopchenko[14], U.Trevisan[5], C.Troncon[18], F.Verbeure[1], J.V.Yarba[8], G.Zumerle[10]

ABSTRACT

Bose-Einstein correlations among identically charged pions produced in *pp* collisions at 400 GeV/c were studied using the EHS spectrometer. Employing the Lorentz invariant Goldhaber parametrization, the average radius and the strength parameter of incoherence of pion emitting region were determined as a function of the momentum, the transverse momentum, the longitudinal momentum and the rapidity of pions. A decrease of the radius with increasing momentum of pions was observed. A study of Bose-Einstein correlations in terms of directional dependence with respect to the beam axis was presented.

Tokyo Metropolitan College of Allied Medical Sciences, Higashi-ogu 7-2-10, Arakawa-ku, Tokyo 116, Japan
1 Inter-University Institute for High Energies, Brussels, and Dep. of Physics, Universitaire Instelling Antwerpen, B-2610 Wilrijk, Belgium
2 Institut fur Hochenergiephysik D-15735 Berlin-Zeuthen, Germany
3 Tata Institute of Fundamental Research, 400005 Bombay, India
4 CERN, European Organization for Nuclear Research, CH-1211 Geneva 23, Switzerland
5 INFN and University of Genova, I-16146 Genova, Italy
6 CIEMAT-JFN, E-28009 Madrid, Spain
7 University of Mons, B-7000 Mons, Belgium
8 Nucl. Phys. Institute, Moscow State University, SU-119899 Moscow, Russian Federation
9 Dep. of Nucl. Phys., Oxford Univ., Oxford OX1 3RH, United Kingdom
10 INFN and University of Padua, I-35131 Padua, Italy
11 LPNHE, University of Paris VI,F-75230 Paris, France
12 INFN and University of Rome, I-00185 Rome, Italy
13 Centro Brasileiro de Pesquisas Fisicas, 22290 Rio de Janeiro, Brasil
14 Institute for High Energy Physics, Serpukhov, SU-142284 Protvino, Russian Federation
15 CRN High-Energy Phys. Div., and University Louis Pasteur, Strasbourg-C, France
16 Dep. of Physics, University of Stockholm, S-11346 Stockholm, Sweden
17 Dep. of Physics, Tokyo Metropolitan University, Minami Ohsawa, Hachioji, Tokyo 192-03, Japan
18 INFN and University of Trieste, I-34100 Trieste, Italy
19 IHEP, A-1050 Wien, Austria

Key words
Bose-Einstein correlations, *pp* collisions, Multiparticle production, High energy physics

1. Introduction

Bose-Einstein correlations between identically charged bosons produced in elementary particle collisions or nuclear collisions, manifest themselves as an enhanced probability for those bosons to be emitted with small relative momenta in comparion with the uncorrelated case. These are interference effects due to Bose-Einstein symmetrization required for the multiboson wave function, which is the analogue of a second order interference phenomenon of photons [1,2]. They have been led to significant theoretical developments [3-10], and have been applied in particle physics to study the space-time structure of the region from which particles are produced. The first experimental evidence of the Bose-Einstein correlations in particle physics was shown by Goldhaber et al. in $\bar{p}p$ annihilations at 1.05 GeV/c [11]. A review of the present status of experimental data together with the theoretical descriptions of the correlations is presented in [12].

Recent studies of Bose-Einstein correlations for like-sign pions produced in $\gamma\gamma \rightarrow 3\pi^+ 3\pi^-$ reactions at the PETRA e^+e^- storage ring indicate a fully chaotic source of pions [13,14]. Similar studies in e^+e^- annihilations and hadron-hadron collisions yield results consistent with a partially chaotic source [12]. This difference of chaoticity may suggest different production mechanisms. Bose-Einstein correlations between like-sign charge track pairs in e^+e^- annihilation hadronic events at center-of-mass energy around the Z^0 peak at LEP were studied by OPAL [15] and ALEPH [16] collaborations, showing no significant variation in comparison with those of e^+e^- annihilations at lower energies.

In order to study a production mechanism, higher order Bose-Einstein correlations up to fifth order in $\bar{p}p$ collisions were analyzed with methods from quantum optics using UA1 data at $\sqrt{s} = 630$ and 900 GeV [17]. Bose-Einstein correlations in ultrarelativistic nucleus-nucleus collisions were measured to understand the underlying dynamics as well as to observe a possible signal of the quark-gluon plasma [18,19].

It is therefore of interest to study systematically pion correlations in *pp* collisions. In our earlier publication [20], we studied Bose-Einstein correlations of $\pi^\pm\pi^\pm$ pairs with respect to dependences on momentum, charged particle multiplicity and particle density of secondary pions as well as those of $\pi^\pm\pi^\pm\pi^\pm$ triplets and $K^\pm K^\pm$ pairs in *pp* collisions at 400 GeV/c ($\sqrt{s}$=27.4 GeV), in which a decrease of the average radius of the interaction region with increasing momenta of secondary pions was observed in terms of the Kopylov-Podgoretskii parametrization. In this paper, we extend this analysis to study of the correlations in terms of the Lorentz invariant Goldhaber parametrization with respect to their dependences on momentum, transverse momentum, longitudinal momentum and rapidity of secondary pions. Also presented is a study of directional dependence of the Bose-Einstein correlations. A possible influence of Bose-Einstein correlations of $\pi^\pm\pi^\pm$ pairs on spectra of $\pi^+\pi^-$ pairs is discussed.

This paper is organized as follows. A description of the data sample used in the present analysis is given in Sect.2. A procedure of data analyses and results obtained are given in Sect.3, and discussions on our results are made in comparison with other experiments in Sect.4. The conclusions are summarized in Sect.5. Finally some comments on the reference sample are presented in the appendix.

2. Data Sample

The present analysis was done using the data obtained in the NA27 experiment performed at CERN-SPS with the EHS spectrometer and the small Lexan hydrogen bubble chamber LEBC, which were exposed to a proton beam of 400 GeV/c [21]. The main goal of the experiment was to study the production and decay properties of charmed hadrons [22].

For the bulk of the events where no charm decay candidate was observed within LEBC, the bubble chamber pictures were not measured but the coordinates of the primary interactions and their charged particle multiplicities were recorded [23]. These data could be used in conjunction with the EHS spectrometer information for reconstruction of the tracks of secondaries. In the present analysis, we used 472,000 interactions within the limit of the LEBC fiducial volume, for which the LEBC and EHS spectrometer information are as complete as possible. Details on data processing are published in [23,24]. We briefly describe here the aspects which are more relevant for the present analysis.

Data were taken by a simple interaction trigger which required three or more hits in each of the two single plane trigger wire chambers positioned just downstream of LEBC. A trigger loss is mainly found at low multiplicities [21]. Therefore, for the present analysis, we selected events with

$$6 \leq \text{charged multiplicity} \leq 30 \tag{1}$$

in which the trigger losses were negligibly small.

The geometrical acceptance of the EHS spectrometer for charged particles covers almost 100% of the forward center of mass hemisphere, the Feynman variable $X_F (= p_{\parallel}^{*}/p^{*}_{max}) > 0$ [23,24]. The average error on the momentum of the reconstructed tracks is $\langle \triangle p/p \rangle \leq 1.5\%$ [24]. The efficiency of track reconstruction depends on kinematical track parameters. It was estimated using a sample of about 16,000 events for which the LEBC pictures were fully measured, that was more than 95% in the $X_F > 0$ region, while very poor for $X_F < 0$ [23]. We used tracks of events which satisfied the condition

$$0 \leq X_F \leq 0.5. \tag{2}$$

The upper bound 0.5 was imposed to reject tracks due to diffraction dissociation and high energy protons in the forward direction. The condition (2) also reduces biases due to the violation of energy and momentum conservation when we make reference samples by the mixed events technique (see below). In the following analysis, each two-particle combination was given a weight equal to the product of the inverse of the efficiency of track reconstruction of a single particle, which was parametrized using a smooth function of the kinematical track parameters [22]. The X_F distribution of tracks which satisfied the conditions (1) and (2) is given in Fig. 1(a). It shows that we used secondaries of the central c.m. region for the present study.

The charged particles were identified by a large pictorial drift chamber ISIS, which provided up to 320 independent measurements of dE/dX for each particle traversing the chamber [21]. For a given track, the probabilities of each mass hypothesis (electron, π, K and proton) were calculated comparing the measured and expected ionization for each mass. The mass hypothesis giving the largest probability was selected if it was larger than 10% with more than 100 independent measurements in the momentum range 5-45 GeV/c; otherwise the pion mass was assumed. Details about the geometrical acceptance and the effi-

ciency of ISIS are given in [20,24]. Electron-hadron separation for charged tracks was also performed using the information of the energy released in the gamma detectors together with the momentum measured in the spectrometer[22].

Since the two magnets of the EHS spectrometer are placed at 2.7m and 18m downstream of LEBC, trajectories of secondaries produced in the bubble chamber are almost straight lines. Therefore an e^+e^- pair from a converted photon, which is close to the interaction vertex in LEBC, is reconstructed as two tracks of opposite charge with a small opening angle. To eliminate these tracks in our analysis, we imposed the criterion that a pair of tracks of opposite charge should have an opening angle θ,

$$\theta > 2 \text{ mrad} \tag{3}$$

in the lab. system. Distributions of opening angles of well identified e^+e^- pairs by ISIS and the gamma detectors showed that more than 95% of e^+e^- pairs from converted photons were eliminated by this criterion. In the case of identically charged particles, we also imposed the criterion (3) to remove one of two tracks which was a possible close ghost track caused by the limited two-track resolution of the spectrometer. Figs. 1(b),(c) and (d) show distributions of the polar angle $\cos\theta_{cm}$, the momentum and the rapidity of pions with respect to the beam axis in the center of mass system used in the present analysis.

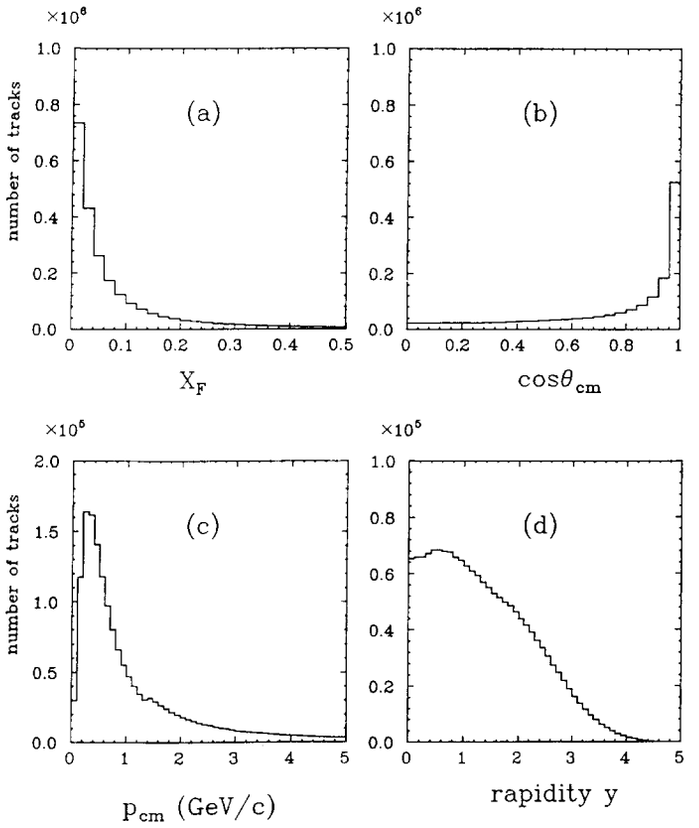

Fig.1 Distributions of (a) the Feynman variable X_F, (b) the polar angle $\cos\theta_{cm}$, (c) the momentum p_{cm} and (d) the rapidity y for secondary tracks in center of mass system used in the present analysis.

3. Data Analysis

3.1 PARAMETRIZATION

The phenomenon of Bose-Einstein correlation is usually studied in terms of the ratio R of the joint probability for a pair of identical particles to be emitted, $P(p_1, p_2)$, to the product $P(p_1)P(p_2)$ of the single particle probabilities, where p_1 and p_2 are the four momenta of the two particles.

$$R=\frac{P(p_1, p_2)}{P(p_1)P(p_2)} \tag{4}$$

In order to evaluate this ratio experimentally, R of eq.(4) can be rewritten as

$$R(X)=\frac{P(X)_{real}}{P(X)_{ref}} \tag{5}$$

where X is a kinematical quantity representing two-particle correlations, namely Q^2 defined below. $P(X)_{real}$ and $P(X)_{ref}$ are probabilities giving X determined with real data and reference samples respectively. Both of them are normalized to be unity within a limited region of X. Uncorrelated particles of reference samples described in the next section allows us to regard $P(X)_{ref}$ as $P(p_1)P(p_2)$ in eq.(4).

A Lorentz-invariant parametrization, which is commonly used in e^+e^- and lepton-hadron as well as hadron-hadron reactions, was introduced by Goldhaber et al.[11]:

$$R(Q^2)=1+\exp(-r^2Q^2) \tag{6}$$

with the negative of the invariant four momentum transfer squared

$$Q^2=-(p_1-p_2)^2=M^2_{12}-4m^2$$

where p_1, p_2 are the four momenta of the particles 1,2, M_{12} is the effective mass of the two particle system and m the mass of the particle. The form (6) corresponds to a Gaussian shape of width r for the particle emission.

The formula (6) was derived assuming totally incoherent production of identical bosons, which gives the maximum interference effect $R=2$ for $p_1=p_2$. However, the maximum effect observed in most experiments is smaller than $R=2$, that is, the interference effect is partial. In order to take care of the partial interference, Deutschmann et al.[25] introduced a strength parameter λ, which was often interpreted as a measure of the incoherence or chaoticity of the boson emitters, namely $0\leq\lambda\leq1$. Actual theoretical understanding is that the interference effect among identical bosons can be smaller than its maximum because of several effects such as resonance production, Coulomb and strong interactions between the bosons, and coherent production[12]. Introducing this strength paremeter λ, we employed the following formula

$$R(Q^2)=C[1+\lambda\exp(-r^2Q^2)]\cdot(1+\delta Q^2), \tag{7}$$

In this equation, C is a normalization constant and δ takes into account of the slow variation of R with Q^2. Numerical values of C and δ are given together with r by fit to the experimental data. The quantity $R(Q^2)$ for $\pi^{\pm}\pi^{\pm}$ ($\pi^{+}\pi^{-}$) pairs is obtained experimentally evaluating ratio of normalized Q^2 distributions of $\pi^{\pm}\pi^{\pm}$ ($\pi^{+}\pi^{-}$) of the real data to those of $\pi^{\pm}\pi^{\pm}$ ($\pi^{+}\pi^{-}$) of a reference sample.

3.2 REFERENCE SAMPLE

As seen from the denominator $P(p_1)P(p_2)$ of eq. (4), an ideal reference sample should be free from any undesirable correlations such as resonances or the Bose-Einstein correlations, while representing the kinematical phase space of the studied sample. Well-known reference samples so far are $(+-)$ combinations of two charged particles in the same event of real data, Monte Carlo events and mixed events. In case of $(+-)$ combination of real data, they include resonances which may disturb partially distributions of $R(X)$. In case of Monte Carlo events, it is not known to what extent resonance production is correctly described especially for $\eta'(958)$ production [24]. To make the reference sample as close to the ideal one as possible, we employed the mixed event technique.

In addition to the criterion (1) for the charged multiplicity, we selected events which have more than three charged tracks well reconstructed in the interval $0 \leq X_F \leq 0.5$. In order to minimize an amount of violation of energy and momentum conservation in the mixed event technique, we grouped the events into configurations which were defined both by the charged particle multiplicity group of (6,7,....30) and by the number of charged tracks (4,5,....30) reconstructed in the interval $0 \leq X_F \leq 0.5$, namely 25·27 configurations. The momentum vectors of particles of the event were stored in a data bank of the corresponding configuration. A reference sample was formed by combining randomly particles of different events in the data bank of this configuration, in which fifty preceding events of the same configuration were stored. It did not contain two tracks from a same real event. Events stored in the data bank were updated taking the new one and dropping the old one in computing successively. The criterion (3) for the opening angle was imposed in the analysis of the reference sample too.

For each real event of a given configuration, a corresponding reference sample was formed simultaneously. Q^2 distributions of a real event were calculated using tracks in $0 \leq X_F \leq 0.5$, and at the same time, those of the reference sample were calculated using tracks in the same interval. Q^2 distributions of real events and reference samples were accumulated separately for all events, and finally $R(Q^2)$ was evaluated using the relation (5).

Fig.2 (a) and 2 (b) show the ratios $R(Q^2)$ for $\pi^{\pm}\pi^{\pm}$ and $\pi^{+}\pi^{-}$ pairs, respectively, in which a number of pairs of Q^2 distributions in the region of $0.2 < Q^2 < 1.0\,(GeV/c)^2$, where the Bose-Einstein correlations are negligible, is normalized to unity in the real data and the reference sample. A significant enhancement for $\pi^{\pm}\pi^{\pm}$ pairs is obseved in the region $Q^2 < 0.08\,(GeV/c)^2$ in Fig.2 (a) in contrast to the flat distributions ($R(Q^2) \sim 1$) in the region $0.08 < Q^2 < 1.0\ (GeV/c)^2$. On the other hand, $R(Q^2)$ for $\pi^{+}\pi^{-}$ pairs in Fig.2 (b) shows a small dip structure in the region $Q^2 < 0.05\,(GeV/c)^2$ as well as a small enhancement at $Q^2 \sim 0.16\ (GeV/c)^2$ due to K^0_S decays close to the primary interaction vertex and that at $Q^2 \sim 0.51\ (GeV/c)^2$ due to ρ^0 decays. We discuss these structures in the appendix. A fit to the data of Fig.2 (a) with the Goldhaber parametrization [7] gives $C = 0.99 \pm 0.01$, $\lambda = 0.39 \pm 0.01$, $r = 1.21 \pm 0.03$ (fm), $\delta = 0.03 \pm 0.01$ which are in good agreement with those obtained in our earlier publication [20].

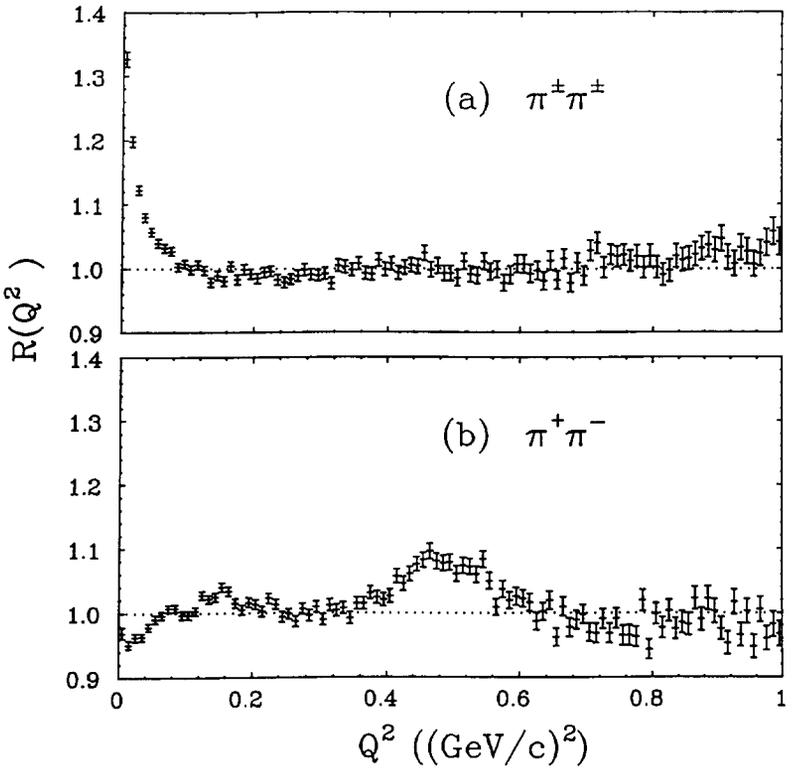

Fig.2 The ratios $R(Q^2)$ of pion pairs (a) for $\pi^+\pi^+$ combinations, and (b) for $\pi^+\pi^-$ combinations. In both cases, a number of pairs of Q^2 distributions in region of $0.2< Q^2 <1.0$ $(GeV/c)^2$ is normalized to unity in the real data and the reference sample. In the case of $\pi^+\pi^-$ combinations, the regions $0.12< Q^2 <0.2$ $(GeV/c)^2$ and $0.4< Q^2 <0.6$ $(GeV/c)^2$ are excluded in the normalization to get rid of K^0_S and ρ^0 respectively.

3.3 PION MOMENTUM DEPENDENCE

We have studied the dependence of the pion source radius r and the strength paremeter λ on the momentum of pions p_{cm} in the center of mass system. We evaluated the ratios $R(Q^2)$ for pion pairs in the momentum intervals of p_{cm} of 0-0.2, 0.2-0.4, 0.4-0.6 and 0.6-1.0 GeV/c for both pions. The ratios $R(Q^2)$ for $\pi^{\pm}\pi^{\pm}$ combinations of these momentum intervals are shown in Fig.3.

Curves in Fig.3 are the ones fitted with the Goldhaber parametrization (7). The essential result of this study is summarized in Fig.6 and Table 1. This figure shows a decrease of the source radius r with increasing pion momentum, which implies that energetic pions are more likely emitted from a source of small radius in comparison with that of less energetic pions. In contrast with this behavior, values of the strength parameter λ are increasing with increasing pion momentum.

Fig.4. shows the ratios $R(Q^2)$ for $\pi^{\pm}\pi^{\pm}$ pairs in the transverse momentum intervals of p_T of 0-0.2, 0.2-0.4 and 0.4-0.6 GeV/c for both pions. Curves in Fig.4 are the ones fitted with the Goldhaber parametrization (7). Fitted parameters are summarized in Fig.6 and Table 1. Results obtained after a similar analysis for $\pi^{\pm}\pi^{\pm}$ pairs in the longitudinal momentum intervals of p_L of 0-0.2, 0.2-0.4, 0.4-0.6 and 0.6-1.0 GeV/c are shown in Fig.5 and are summarized in Fig.6 and Table 1.

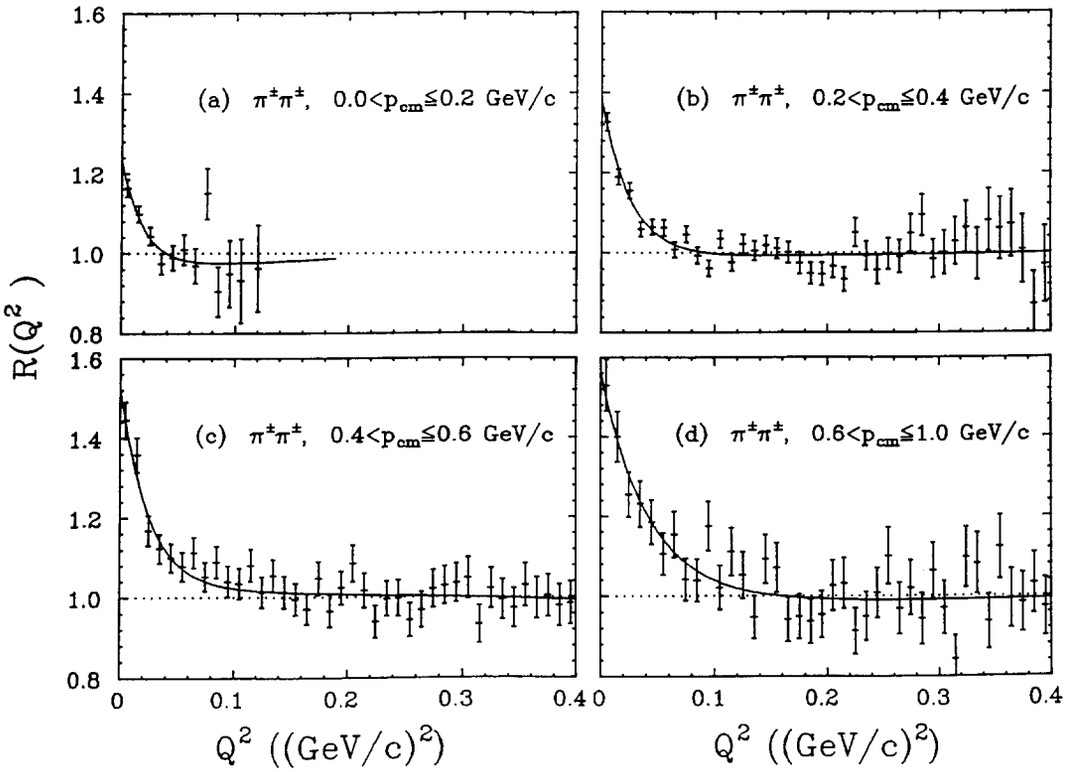

Fig.3 The ratios $R(Q^2)$ for $\pi^{\pm}\pi^{\pm}$ pairs for both of pions with the momentum p_{cm} in the intervals of (a) 0.0-0.2, (b) 0.2-0.4, (c) 0.4-0.6, and (d) 0.6-1.0 (GeV/c). A number of pairs of Q^2 distributions in region of $0.05 > Q^2$ $(GeV/c)^2$ in (a) or $0.2 < Q^2 < 0.4$ $(GeV/c)^2$ in (b), (c) and (d) is normalized to unity in the real data and the reference sample. The curves are fits to the Goldhaber parametrization (7).

Table 1 p_{cm}, p_T, p_L dependence of the parameters fitted with eq. (7) to $R(Q^2)$ data.

p_{cm} GeV/c	C	λ	r fm	δ (GeV/c)^2	χ^2/NDF
.0−.2	0.96±0.11	0.28±0.14	1.42±0.40	0.15±1.55	12/8
.2−.4	0.99±0.02	0.40±0.03	1.24±0.10	0.03±0.09	47/36
.4−.6	1.02±0.02	0.50±0.06	1.25±0.14	-0.06±0.07	42/46
.6−1.	0.98±0.07	0.59±0.09	0.96±0.15	0.03±0.23	39/36
p_T GeV/c	C	λ	r fm	δ (GeV/c)^2	χ^2/NDF
.0−.2	0.99±0.02	0.37±0.02	1.31±0.09	0.03±0.09	34./30
.2−.4	0.98±0.02	0.50±0.03	1.01±0.06	0.06±0.05	42./41
.4−.6	0.98±0.05	0.75±0.12	1.08±0.14	0.01±0.17	42./36
p_L GeV/c	C	λ	r fm	δ (GeV/c)$^{-2}$	χ^2/NDF
.0−.2	0.97±0.01	0.35±0.03	1.42±0.06	0.11±0.02	38./44
.2−.4	0.99±0.04	0.37±0.04	1.10±0.17	0.02±0.14	41./38
.4−.6	0.98±0.03	0.54±0.08	1.38±0.18	0.07±0.14	36./35
.6−1.	1.01±0.06	0.52±0.10	0.99±0.17	-0.05±0.21	45./41

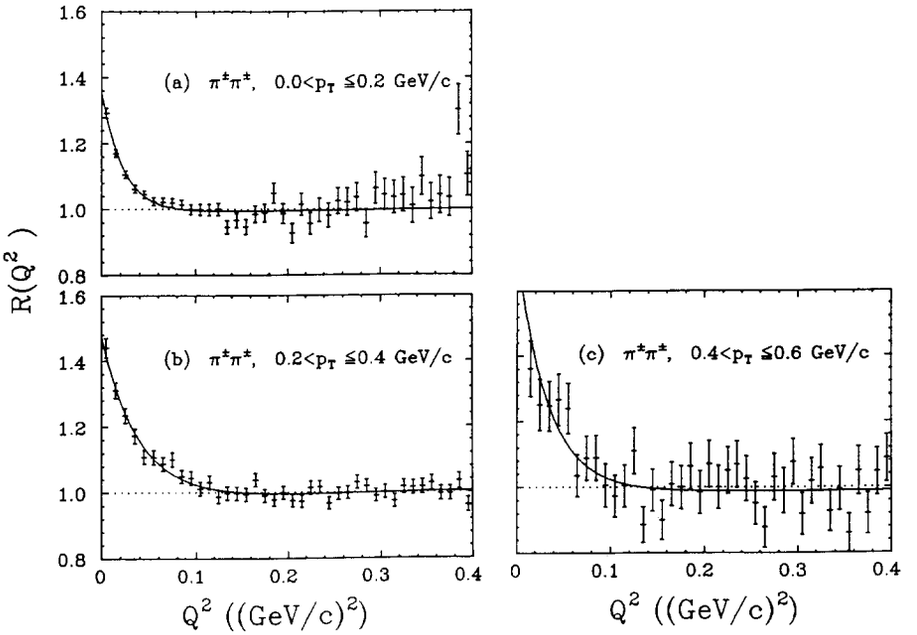

Fig.4 The ratios $R(Q^2)$ for $\pi^+\pi^+$ pairs for both of pions with the transverse momentum p_T in the intervals of (a) 0.0-0.2, (b) 0.2-0.4 and (c) 0.4-0.6 (GeV/c). A number of pairs of Q^2 distributions in region of $0.2< Q^2 <0.4$ $(GeV/c)^2$ is normalized to unity in the real data and the reference sample. The curves are fits to the Goldhaber parametrization (7).

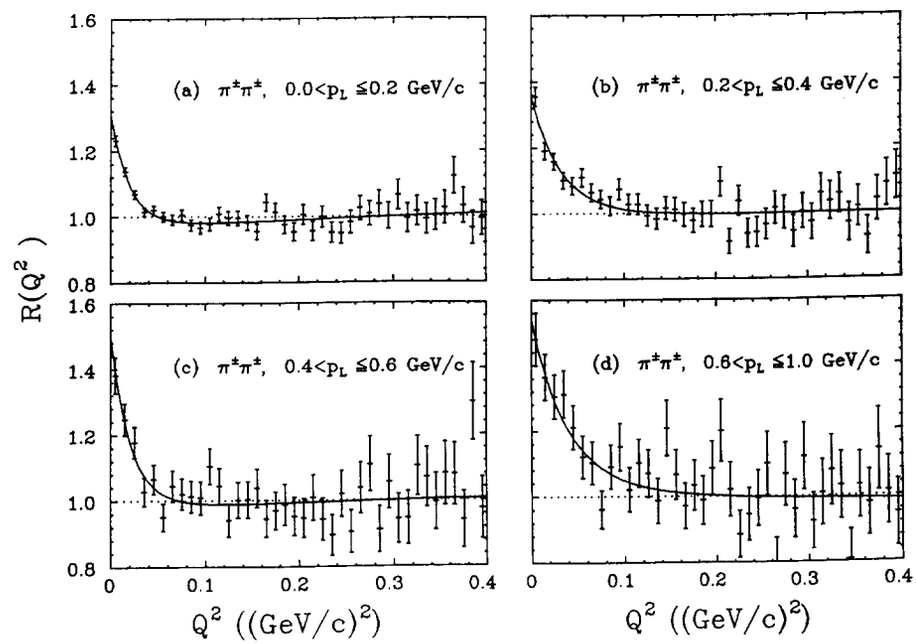

Fig.5 The ratios $R(Q^2)$ for $\pi^+\pi^+$ pairs for both of pions with the longitudinal momentum P_L in the intervals of (a) 0.0-0.2, (b) 0.2-0.4, (c) 0.4-0.6, and (d) 0.6-1.0 (GeV/c). A number of pairs of Q^2 distributions in region of $0.2 < Q^2 <0.4$ $(GeV/c)^2$ is normalized to unity in the real data and the reference sample. The curves are fits to the Goldhaber parametrization (7).

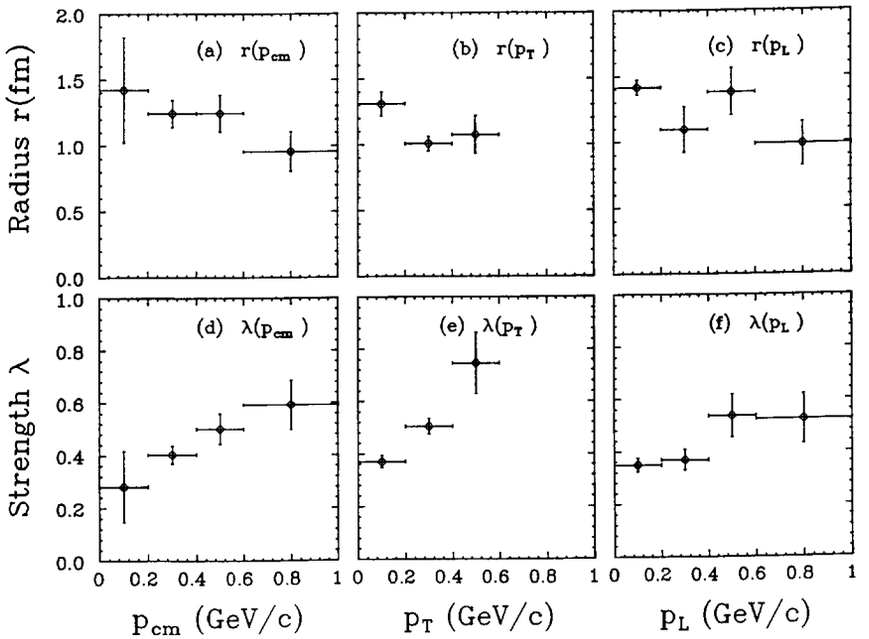

Fig.6 Summary of the source radius r and the strength parameter λ of the Goldhaber parametrization (7) determined experimentally as a funtion of p_{cm}, p_T and p_L.

3.4 DIRECTIONAL DEPENDENCE

In order to study the directional dependence of Bose-Einstein correlations, we employed the polar angle $cos\,\theta_{cm}$ of emitted pions and the polar angle $cos\,\theta\ (\Delta\mathbf{p})$ of the momentum difference $\Delta\mathbf{p}(=\mathbf{p}_1-\mathbf{p}_2)$ for $\pi^{\pm}\pi^{\pm}$ pairs with respect the beam axis in the center of mass system. In the first case, the ratios $R(Q^2)$ were evaluated using pions emitted within the directions $0< cos\,\theta_{cm} \leq 0.7$ and using those in $0.7< cos\,\theta_{cm} \leq 1.0$ separately. Fig.7 shows the ratios $R(Q^2)$ thus obtained for $\pi^{\pm}\pi^{\pm}$ pairs. Curves in these figures are those drawn with the fitted parameters of the Goldhaber parametrization (7), which are summarized in Table 2. One can observe no significant difference of the fitted parameters between the two fits.

In the second case, use has been made of the fact that r is the dimension parallel to $\Delta\mathbf{p}$ [26]. Indeed, a possible dependence of r on the angle $\theta\ (\Delta\mathbf{p})$ was reported by the AFS collaboration [26]. We studies the Bose-Einstein correlations in terms of $\theta\ (\Delta\mathbf{p})$. Fig.8 shows distributions of $\cos\theta\ (\Delta\mathbf{p})$ for $\pi^{\pm}\pi^{\pm}$ pairs used in the analysis. The ratios $R(Q^2)$ were evaluated using $\pi^{\pm}\pi^{\pm}$ pairs with $0< \cos\theta\ (\triangle\mathbf{p}) \leq 0.7$ and using those with $0.7< cos\,\theta\ (\Delta\mathbf{p}) \leq 1.0$ separately. Fig.9 shows the ratios $R(Q^2)$ thus obtained, and the fitted parameters of the Goldhaber parametrization (7) are summarized in Table 2. One can observe no significant difference of the fitted parameters between the two fits, which is consistent with that of the case of $cos\,\theta_{cm}$.

It is interesting, in the picture of the hydrodynamical model, to study a dependence of the longitudinal source radius r on the rapidity [27]. The ratios $R(Q^2)$ were evaluated using $\pi^{\pm}\pi^{\pm}$ pairs in various rapidity intervals of 0-1, 1-2 and 2-3. They are shown in Fig.10 together with fitted curves. The fitted parameters are summarized Fig.13 and Table 3. Figs.11 and 12 show the ratios $R(Q^2)$ of $\pi^{\pm}\pi^{\pm}$ pairs in

various rapidity intervals for the pairs of $0< cos\,\theta\,(\Delta\mathbf{p}) \leq 0.7$ and $0.7< cos\,\theta\,(\Delta\mathbf{p}) \leq 1.0$ respectively. Curves in these figures are fitted ones, and the fitted parameters are summarized in Fig.13 and Table 3. A result summarized in Fig.13 is consistent with no significant dependence of the pion source radius r and the strength parameter λ on the rapidity in both cases of $0< cos\,\theta\,(\Delta\mathbf{p}) \leq 0.7$ and $0.7< cos\,\theta\,(\Delta\mathbf{p}) \leq 1.0$. Note that the rapidity intervals 0-1, 1-2 and 2-3 cover the intervals of momentum p_{cm} of 0~1, 0.3~2, and 0.5~5 GeV/c respectively as shown in Fig.14.

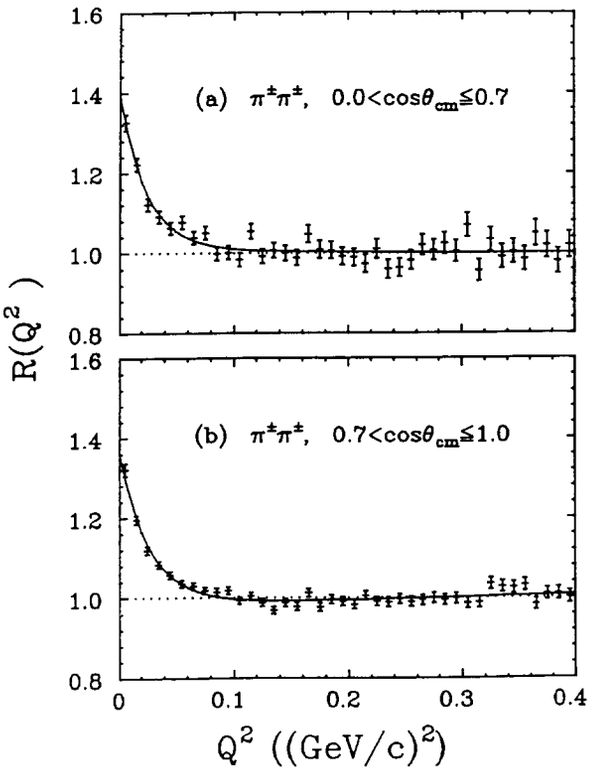

Fig.7 The ratios $R(Q^2)$ for $\pi^+\pi^+$ pairs for pions in region of $cos\,\theta_{cm}$. (a) $0< cos\,\theta_{cm} \leq 0.7$ and (b) $0.7< cos\,\theta_{cm} \leq 1.0$. A number of pairs of Q^2 distributions in region of $0.2< Q^2 <0.4$ $(GeV/c)^2$ is normalized to unity in the real data and the reference sample. The curves are fits to the Goldhaber parametrization (7).

Table 2 $cos\,\theta_{cm}$, $cos\,\theta\,(\Delta\mathbf{p})$ dependence of the parameters fitted with eq. (7) to $R(Q^2)$ data.

$cos\,\theta_{cm}$	C	λ	r fm	δ (GeV/C)^2	χ^2/NDF
.0−.7	1.01±0.01	0.38±0.03	1.26±0.09	−0.01±0.05	50./38
.7−1.	0.98±0.01	0.39±0.02	1.20±0.05	0.07±0.03	51./36
$cos\,\theta\,(\Delta\mathbf{p})$	C	λ	r fm	δ (GeV/C)^2	χ^2/NDF
.0−.7	1.02±0.01	0.35±0.02	1.26±0.06	−0.08±0.03	40./36
.7−1.	0.98±0.01	0.42±0.02	1.25±0.05	0.09±0.03	74./36

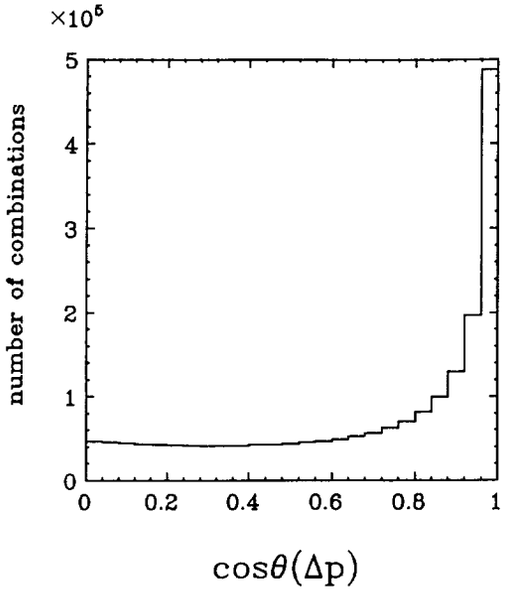

Fig.8 Distributions of the polar angle $\cos\theta(\Delta\mathbf{p})$ of the momentum difference $\Delta\mathbf{p}$ with respect to the beam axis in the center of mass system for $\pi^+\pi^+$ pairs.

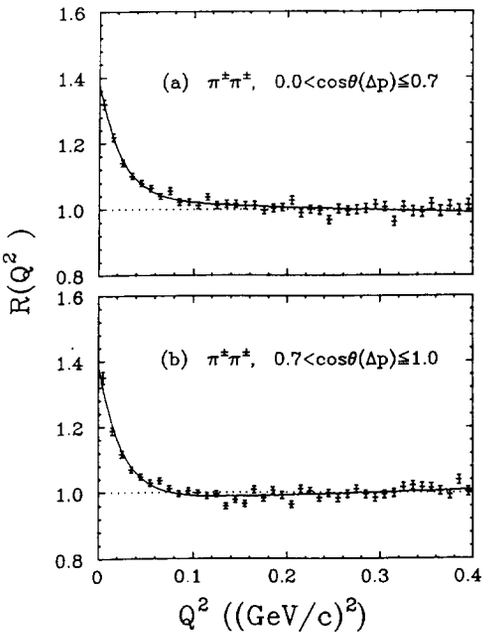

Fig.9 The ratios $R(Q^2)$ for $\pi^+\pi^+$ pairs with the polar angle of (a) $0<\cos\theta(\Delta\mathbf{p})\leq 0.7$ and (b) $0.7<\cos\theta(\Delta\mathbf{p})\leq 1.0$. A number of pairs of Q^2 distributions in region of $0.2<Q^2<0.4\,(GeV/c)^2$ is normalized to unity in the real data and the reference sample. The curves are fits to the Goldhaber parametrization (7).

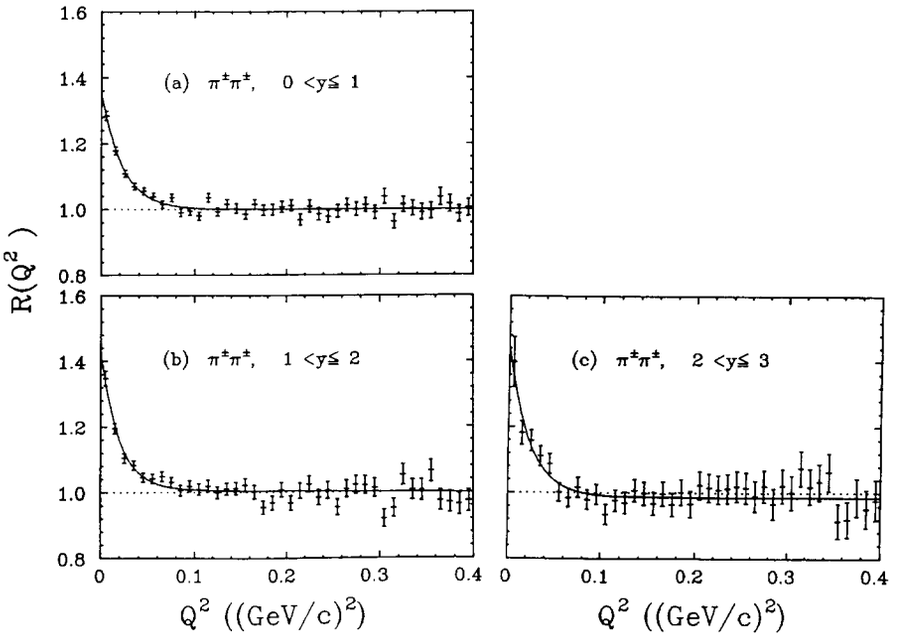

Fig.10 The ratios $R(Q^2)$ for $\pi^+\pi^+$ pairs within the rapidity intervals of (a) $0<y\leq 1$, (b) $1<y\leq 2$ and (c) $2<y\leq 3$. A number of pairs of Q^2 distributions in region of $0.2< Q^2 <0.4$ $(GeV/c)^2$ is normalized to unity in the real data and the reference sample. The curves are fits to the Goldhaber parametrization (7).

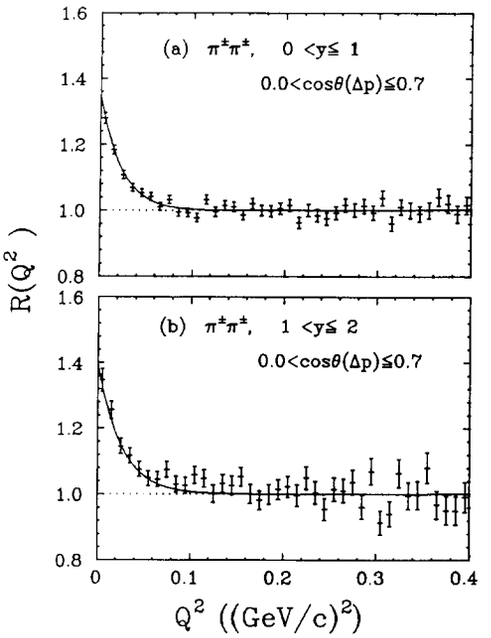

Fig.11 The ratios $R(Q^2)$ for $\pi^+\pi^+$ pairs of $0< \cos\theta(\Delta\mathbf{p}) \leq 0.7$ within the rapidity intervals of (a) $0<y\leq 1$ and (b) $1<y\leq 2$. A number of pairs of Q^2 distributions in region of $0.2< Q^2 <0.4$ $(GeV/c)^2$ is normalized to unity in the real data and the reference sample. The curves are fits to the Goldhaber parametrization (7).

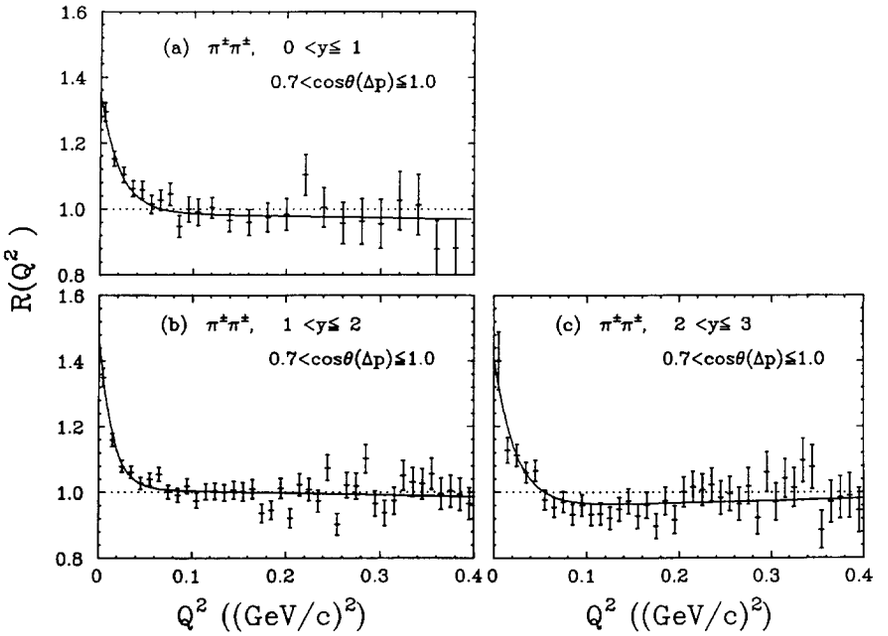

Fig. 12 The ratios $R(Q^2)$ for $\pi^{\pm}\pi^{\pm}$ pairs of $0.7 < \cos\theta(\Delta\mathbf{p}) \leq 1.0$ within the rapidity intervals of (a) $0 < y \leq 1$, (b) $1 < y \leq 2$ and (c) $2 < y \leq 3$. A number of pairs of Q^2 distributions in region of $0.2 < Q^2 < 0.4$ $(GeV/c)^2$ is normalized to unity in the real data and the reference sample. The curves are fits to the Goldhaber parametrization (7). Because of low statistics of data in (a), a bin width in it is twice as large as that of (b) and (c).

Table 3 Rapidity dependence of the parameters fitted with eq. (7) to $R(Q^2)$ data.

rapidity	C	λ	r fm	δ $(\mathrm{GeV/C})^2$	χ^2/NDF
0−1	1.00±0.01	0.35±0.02	1.32±0.07	0.01±0.04	39./36
1−2	1.01±0.01	0.42±0.03	1.42±0.08	-0.02±0.03	79./61
2−3	0.99±0.01	0.47±0.08	1.31±0.12	-0.01±0.05	46./56

$0.0 < \cos\theta(\Delta\mathbf{p}) \leq 0.7$

rapidity	C	λ	r fm	δ $(\mathrm{GeV/C})^2$	χ^2/NDF
0−1	1.00±0.01	0.35±0.02	1.30±0.07	0.02±0.04	39./36
1−2	1.00±0.01	0.40±0.04	1.23±0.11	0.01±0.04	72./61

$0.7 < \cos\theta(\Delta\mathbf{p}) \leq 1.0$

rapidity	C	λ	r fm	δ $(\mathrm{GeV/C})^2$	χ^2/NDF
0−1	0.99±0.03	0.36±0.05	1.38±0.21	-0.05±0.18	12./19
1−2	1.01±0.01	0.46±0.06	1.64±0.16	-0.06±0.07	54./32
2−3	0.95±0.02	0.48±0.09	1.29±0.14	0.08±0.06	53./56

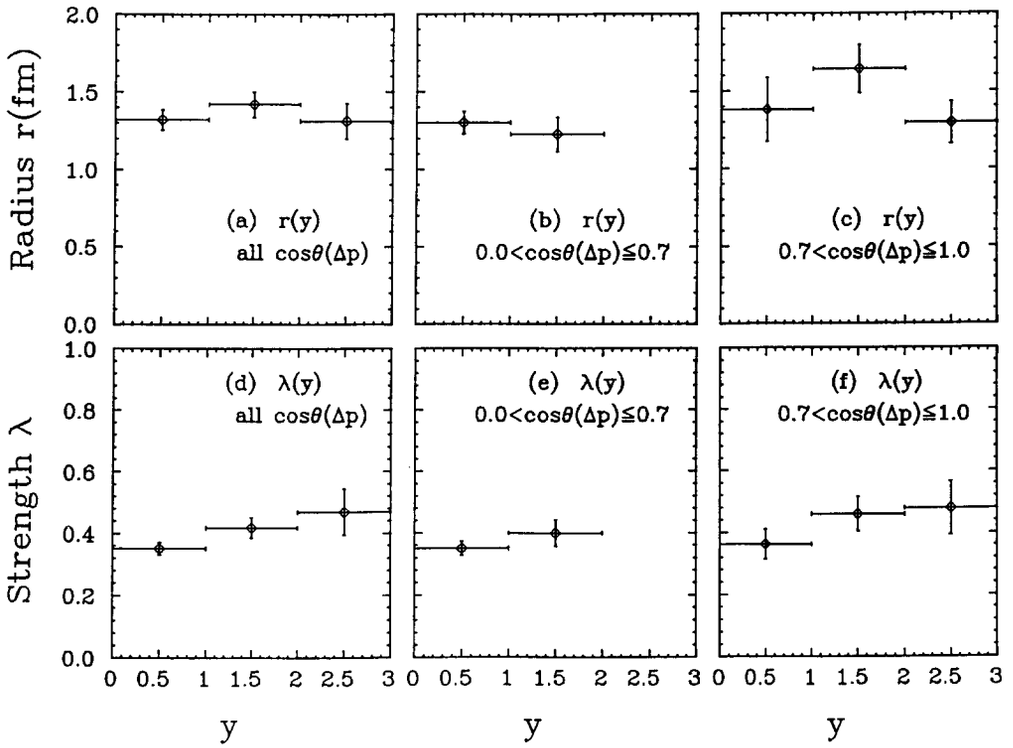

Fig.13 Summary of the source radius r and the strength parameter λ of the Goldhaber parametrization (7) determined experimentally for various rapidity intervals and $cos\,\theta$ ($\Delta \mathbf{p}$) intervals.

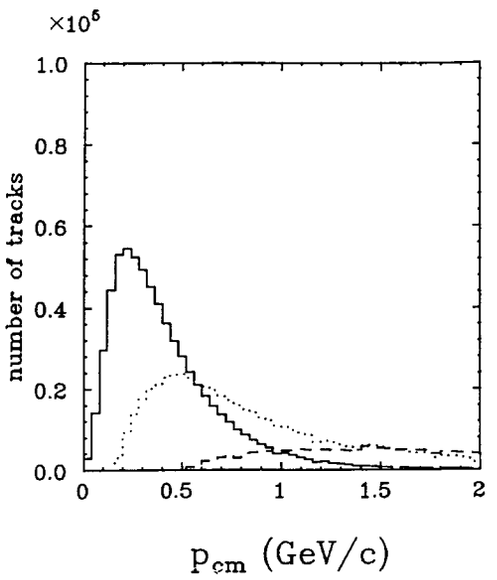

Fig.14 Distributions of the momentum p_{cm} of secondary tracks within the rapidity intervals of $0<y\leq 1$ (solid line), $1<y\leq 2$ (dotted line), and $2<y\leq 3$ (dashed line).

4. Discussion

Since energy and momentum conservation is not taken into account in forming the reference sample events, it is not ideal one. Therefore we control our method by producing a reference sample and evaluating the ratio $R(Q^2)$ for $\pi^+\pi^-$ pairs where the Bose-Einstein correlation is absent. Comparing the ratios $R(Q^2)$ evaluated with $\pi^\pm\pi^\pm$ pairs and $\pi^+\pi^-$ ones, we can estimate possible correlations independent from the charge, which are induced by the method of analysis or by the detector itself. We have studied Bose-Einstein correlations for $\pi^\pm\pi^\pm$ pairs with the reference sample of mixed events described in Sect.3.2, and at the same time, we checked the ratios $R(Q^2)$ for $\pi^+\pi^-$ pairs as shown in [20]. $R(Q^2)$ for $\pi^+\pi^-$ pairs in Fig.2(b) shows a small dip structure in the region $Q^2 < 0.05\ (GeV/c)^2$ as well as a small enhancement at $Q^2 \sim 0.16\ (GeV/c)^2$ due to K^0_S decays and that at $Q^2 \sim 0.51\ (GeV/c)^2$ due to ρ^0 decays. This small dip structure was observed in the ratios $R(q_t)$ of the Kopylov-Podgoretskii parametrization at small q_t region ($q_t < 0.2\ GeV/c$) [20]. This point is discussed in the appendix. Furthermore, momentum spectra of π^+ and π^- are not same in our case as we are dealing with pp interactions. By these reasons, we employed a reference sample of mixed events instead of $\pi^+\pi^-$ combinations of the same event.

Among the many resonances produced, the cascade decays of $\eta'(958)$, $\eta' \rightarrow \pi^+\pi^-\eta$ followed by $\eta \rightarrow \pi^+\pi^-\pi^0$ or $\eta \rightarrow \pi^+\pi^-\gamma$, are known to produce identically charged pions with low Q^2 or q_t values. The influence of the η' decay on charged-pion interferometry in e^+e^- annihilations was studied using the Lund fragmentation model [28]. In an earlier study of Bose-Einstein correlations in pp collisions at 360 GeV/c [29], it was estimated that removal of identically charged pion pairs from η' decays leads to an increase of the radius r by $\sim 4\%$ and a decrease of the strength parameter λ by $\sim 10\%$. In the present work, no such subtraction was done because the η' production cross section is not well known [24].

A correction for the ratio $R(Q^2)$ due to Coulomb interactions is of the order of a few percents for $Q^2 \leq 0.01\,(GeV/c)^2$, and is smaller for large Q^2 [30]. This was neglected in the present analysis.

Our results obtained by means of the Goldhaber parametrization are consistent with a picture of particle emission from a spherically expanding source, which is in agreement with the conclusions of the earlier analysis made by means of the Kopylov-Podgoretskii parametrization with the reference sample slightly different from the present one (see the appendix) [20]. No directional dependence of Bose-Einstein correlation was observed with respect to the angle $\cos\theta\ (\Delta\mathbf{p})$ which agreed with results obtained in the K^+p, π^+p experiment at 250 GeV/c [31] and the μp experiment at 280 GeV/c [32].

The study of rapidity dependence of the Bose-Einstein correlations is important in hydrodynamical theory of multiparticle production through the one-dimensional expansion of the matter along the collision axis. Our result shows no significant dependence of the correlation on rapidity, which is consistent with the result obtained in the pseudorapidity range $|\eta| < 3$ by the UA1 collaboration in $\bar{p}p$ collisions at $\sqrt{s} = 200$-900 GeV [33]. On the other hand the NA35 collaboration observed the Bose-Einstein correlations in heavy-ions collisions exhibiting a marked dependence on the rapidity interval considered [18].

B. Lörstad et al. proposed a model of the longitudinal hydrodynamical flow in particle emission, and they showed that their model is consistent with data of the heavy-ion collisions [27]. It is interesting to point out that their hydrodynamical model does not describe well our results, which is in agreement with their conclusion that the hydrodynamical interpretation of minimum bias pp events at the ISR is inadequate [27].

5. Conclusions

Our results can be summarized as follows.

1) We have observed Bose-Einstein correlations employing the Lorentz invariant Goldhaber parametrization for identically charged pions in soft pp interactions at 400 GeV/c ($\sqrt{s}$=27.4GeV).

2) The pion source radius r decreased and the strength parameter λ increased with increasing the pion momentum p_{cm}. This feature appeared with increasing the transverse momentum p_T as well as p_{cm}.

4) No directional dependence of the Bose-Einstein correlations was observed for pions emitted in subdivided regions defined by the angle $\cos\theta_{cm}$ or $\cos\theta$ ($\Delta\mathbf{p}$).

5) No significant dependence of the Bose-Einstein correlations on the rapidity y was observed in the range $0<y\leq 3$ within our error. No rapidity dependence for pions emitted in subdivided regions defined by the angle $\cos\theta$ ($\Delta\mathbf{p}$) was observed within our error too.

6) It is suitable to employ an event mixing technique instead of $\pi^+\pi^-$ combinations of the same event in making a reference sample in our case.

ACKNOWLEDGEMENTS

We are deeply indebted to the CERN-SPS beam and EHS crews for their support during the preparation and runs of our experiment. Thanks are due to the scanning and measuring staff of the collaborating laboratories for their good work which made this analysis possible. Our thanks are due to Prof. B. Lörstad for his useful suggestions. We wish to acknowledge with gratitude the support of various national funding agencies.

Appendix: Comments on the reference sample

In order to study the dip structure in the region of $Q^2<0.05\,(GeV/c)^2$ in Fig.2(b), we evaluated the ratio $R(Q^2)$ for $\pi^+\pi^-$ pairs rejecting one of two tracks of $\pi^\pm\pi^\pm$ pairs in the region of $0<Q^2<0.05$ $(GeV/c)^2$ of the real data in Fig.2(a) where Bose-Einstein correlations were enhanced. The ratio thus obtained is shown in Fig.15(b) together with that for $\pi^+\pi^-$ pairs with no cut of $\pi^\pm\pi^\pm$ pairs (Fig.15(a)). One can see from this figure that the dip structure in $Q^2<0.05$ $(GeV/c)^2$ in Fig.15(a) somewhat disappeared in Fig.15(b). If we evaluated the ratio $R(Q^2)$ for $\pi^+\pi^-$ pairs rejecting one of two tracks of $\pi^\pm\pi^\pm$ pairs in the region of $0.1<Q^2<0.15$ $(GeV/c)^2$ instead of $0<Q^2<0.05\,(GeV/c)^2$ in Fig.2(a) where Bose-Einstein correlations were negligible, the dip structure in the region of $Q^2<0.05$ $(GeV/c)^2$ appears again as shown in Fig.15(c). This behavior, that is, the dependence of the dip structure of $R(Q^2)$ for $\pi^+\pi^-$ pairs on Q^2 cut of $\pi^\pm\pi^\pm$ pairs was observed too in the ratios $R(q_l)$ for $\pi^+\pi^-$ pairs evaluated in terms of the Kopylov-Podgoretskii parametrization[20], which was not shown in the figure.

This fact implies that the dip structure of the Q^2 distributions of $\pi^+\pi^-$ pairs in the region of $Q^2<0.05$ $(GeV/c)^2$ is due to inherent reflection of the Bose-Einstein correlations of $\pi^\pm\pi^\pm$ pairs. These discussions suggest that the mixed-event technique is more suitable than $\pi^+\pi^-$ combinations of same event in making the reference sample. If we employ a reference sample of the $\pi^+\pi^-$ combinations of same event, where the regions of $0.12<Q^2<0.2$ $(GeV/c)^2$ for K^0_S and $0.4<Q^2<0.6$ $(GeV/c)^2$ for ρ^0 are excluded in the fit, we obtain the pion source radius r of $\sim 7\%$ smaller and the strength parameter λ of

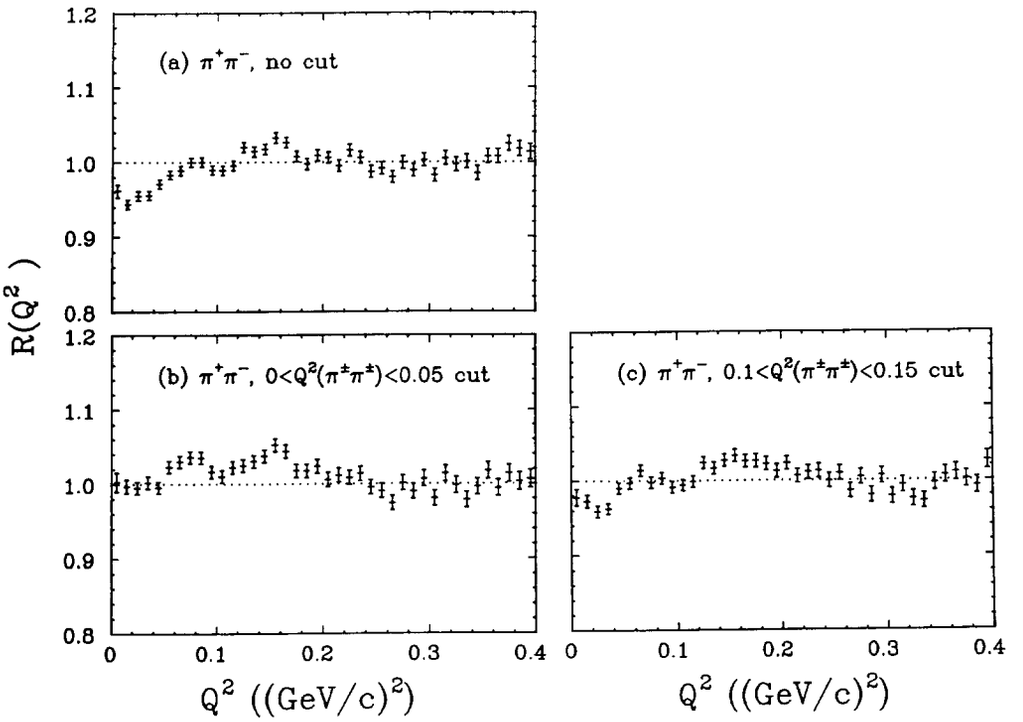

Fig.15 The ratios $R(Q^2)$ for $\pi^+\pi^-$ pairs where (a) no cut in Q^2 distributions of $\pi^+\pi^+$ pairs is imposed, (b) one of $\pi^\pm\pi^+$ of $0<Q^2<0.05$ $(GeV/c)^2$ is rejected and (c) one of $\pi^+\pi^\pm$ of $0.1<Q^2<0.15$ $(GeV/c)^2$ is rejected of the real data. A number of pairs of Q^2 distributions in region of $0.2<Q^2<0.4$ $(GeV/c)^2$ is normalized to unity in the real data and the reference sample.

$\sim$14% larger values for the data of $R(Q^2)$ of $\pi^\pm\pi^\pm$ pairs in comparison with those obtained with a reference sample of the mixed events in Fig.2(a). Fitted parameters for Bose-Einstein correlations with the reference sample of mixed events and those with the reference sample of $\pi^+\pi^-$ combinations of the same event were compared in μp interaction [32], e^+e^- annihilations [16,34] and K^+p, π^+p interactions [31], and thier results did not contradict our above-mentioned argument.

In our earlier work [20], we created a reference sample mixing real events of a given configuration, where the momentum of secondary tracks were expressed with respect to the coordinate system related to the sphericity axis defined by the eigenvectors for the sphericity tensor [35]. As pointed out in [20], reference samples of mixed events expressed in the coordinate system of the sphericity axis and those expressed in the coordinate system fixed in the bubble chamber did not give different results within errors. This fact is understood with our data, in which soft processed of hadron production are dominated and the principal axis of the event is close to the beam axis.

In the present case, the ratio $R(Q^2)$ of $\pi^\pm\pi^\pm$ pairs in the interval of $2<y<3$ gave the parameter δ of significantly larger value than zero in eq.(7) with the reference sample expressed in the coordinate system of the sphericity axis, while it was compatible with zero with the reference sample expressed in the bubble chamber system. This might be caused by ambiguity in evaluation of the eigenvectors for the sphericity tensor for pions with large momentum (see Fig.14), since we are using tracks in the limited region $0 \leq X_F \leq 0.5$. It was preferable to use a reference sample which gave a numerical value of δ close to

zero, therefore we employed the coordinate system fixed in the bubble chamber instead of that of the sphericity axis in making a reference sample in the present analysis.

References

[1] R. Hanbury Brown and R. Q. Twiss, Phil. Mag. **45** (1954) 663

[2] P.L.Knight and L.Allen, Concept of Quantum Optics (Pergamon Press, NY , 1983)

[3] G.I.Kopylov and M.I. Podgoretskii, Sov.J. Nucl. Phys. **15** (1972) 219; **18** (1973) 336

[4] G. Cocconi, Phys. Lett. **49B** (1974) 459

[5] G. N. Fowler and R. M. Weiner, Phys. Lett. **70B** (1977) 201

[6] A.Giovannini and G.Veneziano, Nucl. Phys. **B130** (1977) 61

[7] M. Gyulassy, S. K. Kaufmann, and Lance W. Wilson, Phys Rev. **C20** (1979) 2267

[8] M. Biyajima, Phys. Lett. **92B** (1980) 193

[9] B. Andersson and W. Hofmann, Phys. Lett. **169B** (1986) 364

[10] M. G. Bowler, Z. Phys. C - Particles and Fields **29** (1985) 617; **46** (1990) 305

[11] G. Goldhaber et al., Phys. Rev. **120** (1960) 300

[12] W.A.Zajc, Proc. Conf. on Multiparticle production, Eds.P. Carruthers (World Scientific, Singapore, 1988); D.H. Boal, C-K Gelbke and B.K. Jennings, Rev. Mod. Phys. **62** (1990) 553

[13] CELLO Coll., H.-J.Behrend et al., Phys. Lett. **245B** (1990) 298.

[14] JADE Coll., R.Pust et al., Z. Phys. C - Particles and Fields **51** (1991) 531

[15] OPAL Coll., P.D.Acton et al., Phys. Lett. **267B** (1991) 143.

[16] ALEPH Coll., D.Decamp et al., Z. Phys. C- Particles and Fields **54** (1992) 75

[17] UA1-MINIMUM BIAS Coll., N.Neumeister et al., Phys. Lett. **275B** (1992) 186.

[18] NA35 Coll., A.Bomberger et al., Phys. Lett. **203B** (1988) 320.

[19] WA80 Coll., R.Albrecht et al., Z. Phys. C - Particles and Fields **53** (1992) 225

[20] LEBC-EHS Coll., M.Aguilar-Benitez et al., Z. Phys. C - Particle and Fields **54** (1992) 21

[21] LEBC-EHS Coll., M.Aguilar-Benitez et al., Nucl. Instrum. Methods **A258** (1987) 26

[22] LEBC-EHS Coll., M.Aguilar-Benitez et al., Z. Phys. C - Particle and Fields **40** (1988) 321

[23] Yu.Fisjak et al., Minimum bias events from EHS, Preprint CERN/EP **87-137** (1987)

[24] LEBC-EHS Coll., M.Aguilar-Benitez et al., Z. Phys. C - Particles and Fields **50** (1991) 405

[25] M. Deutschmann et al., Nucl. Phys. **204B** (1982) 333

[26] AFS Coll., T. Åkesson et al., Phys. Lett. **187B** (1987) 420

[27] B.Lörstad and Yu M.Sinyukov, Phys. Lett. **265B** (1991) 159

[28] K. Kulka and B. Lörstad., Nucl. Instrum. Methods **A295** (1990) 443

[29] NA23 Coll., J.L.Bailly et al., Z. Phys. C - Particles and Fields **43** (1989) 341

[30] M. G. Bowler, Phys. Lett. **270B** (1991) 69

[31] NA22 Coll., M. Adamus et al., Z. Phys. C - Particles and Fields **37** (1988) 347

[32] M. Arneodo et al., Z. Phys. C - Particles and Fields **32** (1986) 1

[33] UA1 Coll.,C. Albajar et al., Phys. Lett. **226B** (1989) 410.

[34] MARK II Coll., I. Juričić et al., Phys. Rev. **D39** (1989) 1

[35] NA23 Coll.,J.L. Bailly et al., Phys. Lett. **206B** (1988) 371

400GeV/cの陽子衝突反応における二次パイ中間子のボーズ・アインシュタイン相関の研究

喜多村　章　・　他56名

［要　　旨］

高いエネルギーをもって運動している素粒子がもうひとつの素粒子に衝突すると，パイ中間子等の素粒子を多く生成する。これを二次粒子生成過程という。この過程の機構を解明する方法の一つにボーズ・アインシュタイン相関を用いる方法がある。これは同じ種類の二次粒子の相関を解析することによって，二次粒子が生成される領域の空間的な広がりとその形状の時間的変化を研究するもので，これらの情報から衝突が起こったときの状態を明らかにすることができる。　ここでは入射運動量が400GeV/cの陽子と静止状態の陽子が衝突して発生した二次パイ中間子をヨーロッパ複合型スペクトロメーター（ＥＨＳ）を使って測定して，ボーズ・アインシュタイン相関について研究した。そして素粒子の衝突が起こったときの空間的広がりを測定した。その大きさは，パイ中間子の持つ縦運動量や横運動量の増加によって小さくなっているということが観測されたが，ラピデイテイの変化にはあまり依存しなかった。これらの結果は，衝突で高温状態ができてそれが膨張しながら熱的に冷えてゆく過程で二次粒子が生成されるというように解釈することができる。

［キーワード］
ボーズ・アインシュタイン相関，陽子ー陽子衝突反応，多重粒子生成，
高エネルギー素粒子物理